Korean J. Chem. Eng., **15**(2), 164-176 (1998)

THE EFFECT OF PARTICLE SIZE DISTRIBUTION ON THE OLEFIN POLYMER REACTOR DYNAMICS

Jae Youn Kim*, W. Curt Conne Jr. and Robert L. Laurence†

Department of Chemical Engineering, University of Massachusetts, Amherst, MA 01003
(Received 29 August 1997 • accepted 10 February 1998)

Abstract – Mass and energy balances in a reactor have been derived to study the effect of particle size distribution (PSD) for each reaction mechanism on the reactor dynamics. It was observed that the PSD affects both bed height and particle volume. A feasible region for reactor operation has been calculated by using physical constraints. In a nonisothermal polymerization system, the reactor temperature does not change appreciably as catalyst injection rate increases. A unique steady state solution is found in a gas-phase continuous stirred-bed propylene polymerization reactor. The eigenvalues of the system of equations indicate that the steady state is unstable. A comparison with published data allows the observation that the actual reactor dynamics may be readily explained by using only the PSD derived from a simple reaction mechanism.

Key words: Olefin, Polymerization, Particle Size Distribution, Reactor, Dynamics

INTRODUCTION

Gas phase olefin polymerization processes have developed in the past two decades towards minimizing capital investment in the process, by eliminating separation processes needed for hydrocarbons and polymer products in slurry or solution processes. Continuous stirred-bed reactors (CSBR) and fluidized bed reactors are widely used in gas phase polymerization. The mathematical modeling of fluidized bed reactors is complicated by the mechanics of the fluidization of growing polymer particles. The CSBR affords a simpler description. Here, we developed a mathematical model in order to study the effect of particle size distribution (PSD) on the reactor dynamics. These results may be extended to fluidized bed reactor systems and will be described later.

Very little information has been published on the dynamics of gas phase olefin polymerization reactor systems. Brockmeier and Rogan [1976] modeled a semibatch stirred-bed reactor for gas phase propylene polymerization and obtained the polymer yield and particle size from their model. Choi and Ray [1988] modeled a CSBR for the solid catalyzed gas phase polymerization of propylene. They observed a single unstable steady state at normal operation conditions. However, they assumed the PSD in the reactor to be uniform and ignored the effect of the PSD on the reactor dynamics.

The schematic diagram of a CSBR is shown in Fig. 1. Injected active catalyst is uniformly mixed with polymer particles by a U-shaped anchor agitator. Liquid propylene, which is injected at the bottom of the reactor, instantaneously absorbs the heat of reaction and is vaporized. To regulate the molecular weight of polymer products, a small amount of hydrogen is added to the reactor. The unreacted propylene gas is sent to a condenser and liquefied. This liquefied propylene is recycled to the reactor. Product is withdrawn continuously from the reactor in a cyclone, separating solid polymer from the gas-solid mixture. Since the principal mechanism for the removal of the heat of polymerization is the vaporization of propylene, the reactor must be operated so as to preclude the condensation of propylene. For an equation of state relating

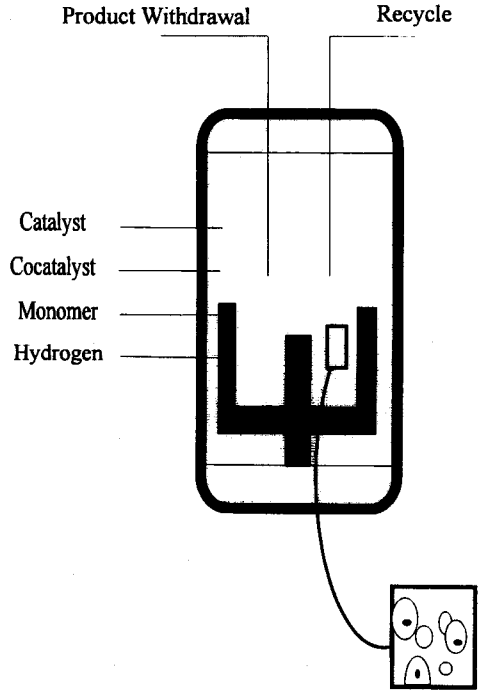

Fig. 1. Schematic diagram of continuous stirred-bed reactor for olefin polymerization.

†To whom all correspondence should be addressed.
*Current Address: Chemicals Research Division, Hanwha Group R/E Center, Taejon 305-345, Korea
E-mail: jaekim@indigo2.hanwha.co.kr

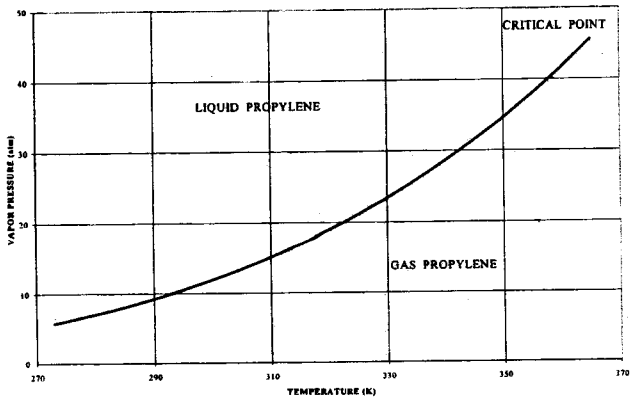

Fig. 2. The relationship between propylene vapor pressure and temperature.

the pressure, temperature and monomer concentration in the reactor, Choi and Ray [1988] used the ideal gas law. This, however, has several limitations and does not represent the state of a real gas. The Redlich-Kwong equation has been used in this work. The vapor pressure expression for propylene [Reid et al., 1987] has been used to calculate the phase diagram of propylene. It shows the state of propylene at a given temperature and pressure which are calculated from the macroscale equations governing the reactor. Fig. 2 shows propylene phase diagram.

THE EQUATIONS GOVERNING THE POLYMERIZATION

Several assumptions taken in this model of a CSBR propylene polymerization include some used in Choi and Ray [1995].

(1) The mixing of gas and solid polymer particle is ideal. The composition of withdrawal product is the same as that of stirred bed.

(2) Catalysts, whose active sites may deactivate during polymerization, are injected continuously to the reactor.

(3) Physical properties, e.g., density, heat capacities of the gas and solid phase, approximated as those of gaseous propylene and polymer, are constant during polymerization.

(4) The Redlich-Kwong equation is used to calculate monomer pressure at a given concentration. The Ideal Gas law is applied to hydrogen in the mixture of gases.

(5) Liquid propylene and hydrogen are fed to the reactor at the same temperature.

(6) The reactor is adiabatic for the nonisothermal model.

(7) The amount of gaseous propylene remaining in the discharged polymer product is negligible.

(8) Monomer does not accumulate in the reactor.

(9) Heat and mass transfer resistances between bulk and particle are negligible.

With these assumptions, the mass and energy balances have been derived for a gas phase polymerization of propylene in a CSBR.

1. Isothermal Systems

Since there are two phases, that is, gas and solid in the reactor, the following definitions will help in developing a representation of the model.

Table 1. Governing equations for isothermal gas phase olefin polymerization in a continuous stirred-bed reactor

$$(1-\delta)\,V_R\frac{dC_M}{dt^*} = q_{Mf} + \frac{C_M}{\rho_{par}}\,q_{cf} - C_M\,Q + r_M\left(1-\frac{C_M}{\rho_{par}}\right)$$

$$(1-\delta)\,V_R\frac{dC_M}{dt^*} = q_{Mf} + \frac{C_M}{\rho_{par}}\,q_{cf} - C_H\,Q + r_{trH} - r_M\frac{C_H}{\rho_{par}}$$

$$\rho_{par}\,V_R\frac{d\delta}{dt^*} = q_{cf} + \rho_{par}\,(1-\varepsilon)Q - r_M$$

$$\rho_{par}\,V_R\,\delta\frac{d\phi_c}{dt^*} = (1-\phi_c)\,q_{cf} + \phi_c\,r_M$$

where $r_M = -V_R\,\delta M_{wM}\int_{V_c}^{\infty} k_p\,[M]_p\,\bar{i}\,f(V)\,dV$

$r_{trM} = -V_R\,\delta M_{wH}\int_{V_c}^{\infty} k_{trH}\,[H_2]_p^{1/2}\,\bar{i}\,f(V)\,dV$

$$\delta = \frac{V_{par}}{V_R} = \frac{V_{par}}{V_{par}+V_g} = \text{Fractional Volume of Stirred-Bed}$$

$$\varepsilon = \frac{v_g}{Q} = \frac{v_g}{v_g + v_{par}} = \frac{\text{Gas Withdrawal Rate}}{\text{Product Withdrawal Rate}}$$

Using the approximation that the rate of monomer consumption is much greater than that of chain transfer to a hydrogen, one may derive the mass balances shown in Table 1.

Hutchinson and Ray [1990] studied the equilibrium monomer sorption to determine the local monomer concentration in the semicrystalline polymer shell that surrounds the catalyst surface. They showed that Stern's correlation fits experimental data very well for light hydrocarbons such as ethylene and propylene and deviates slightly for heavier hydrocarbons. In this work, Stern's correlation is used to calculate monomer concentration at the particle.

$$[M]_p = k_H^*\,P_M$$

$$\log(k_H^*) = -5.38 + 1.08\left(\frac{T_{cr}}{T}\right)^2 \tag{1}$$

where k_H^* is Henry's constant. Though the concentration at the particle is numerically larger than that in the bulk due to unit change (g/cm^3)→(g/cm^{3}par), it is assumed that hydrogen and cocatalyst concentration at the particle are the same as those in the reactor, since the quantities of hydrogen and cocatalyst compared to monomer are small.

2. Nonisothermal Systems

Since the monomer vaporizes as it is injected into the reactor, the energy balance for a gas phase CSBR on olefin polymerization is given by

$$\begin{aligned}[V_R(1-\delta)C_M\,C_{pM} + V_R\,\delta(1-\phi_c)\rho_{par}\,C_{pp}]\frac{dT}{dt^*} \\ = -(q_{Mf}+q_R)\,C_{pM}\,(T-T_{ref}) - (\Delta H_v)\,(q_{Mf}+q_R) \\ + C_{pM1}\,q_R\,(T_R - T_{ref}) + C_{pM1}\,q_{Mf}\,(T_{fM} - T_{ref}) \\ - (-\Delta H_{rxn})\,r_M - (C_{pM} - C_{pp})\,(T - T_{ref})\,r_M\end{aligned} \tag{2}$$

where q_R is the recycle monomer mass flow rate and C_M represents the mass concentration of monomer in the reactor.

In this derivation, the terms containing the catalyst heat capacity and the hydrogen concentration are neglected. Several constraints are required for safe operation of the reactor. The volume fraction δ should be bounded, that is, less than one. Another important constraint comes from phase diagram, which indicates the state of the monomer. Since propylene must be vapor just after being injected into the reactor, there is an acceptable range of pressures at a given temperature. This will be discussed further in the next section. The monomer concentration at the particle is given by Stern's correlation involving monomer pressure, determined using the Redlich-Kwong equation of state in a given bulk monomer concentration. Since this bulk concentration, however, is calculated by solving mass and energy balances, the governing equations and the equation of state should be solved simultaneously.

Floyd et al. [1986a, b, 1987] studied the effect of heat and mass transfer resistance between bulk and particle on polymerization behavior and polymer properties for polymerizations of olefins on a heterogeneous catalyst. They found resistances are negligible except for a highly active and larger initial volume of catalyst. Hutchinson and Ray [1987] studied the possibility of particle ignition and extinction phenomena for olefin polymerization on a heterogeneous catalyst. Overheating was observed at the start of the reaction for gas phase polymerization, when the polymer particle has a high volume to surface area ratio. They observed that as catalyst activity increases, the overheating problem becomes more severe. This result may be important during a start-up of the reactor or grade transition. In this study, it is presumed that there is no particle overheating. These governing equations may be made dimensionless using the dimensional variables and parameters defined in Table 2. Unlike conventional dimensionless variables such as conversion in free-radical polymerization, the monomer and the hydrogen mass concentration are made dimensionless using a reference monomer and hydrogen density. In olefin polymerization, the polymer yield and catalyst residue in the polymer particle are much more important than the conventional term, conversion.

Table 2. Dimensionless variables and parameters for olefin polymerization

$t = \frac{t'}{t_R}$	$t_R = \frac{V_R \rho_{M1}}{q_{Mf}}$	$X_1 = \frac{C_M}{\rho_{Mr}}$	$X_2 = \frac{C_H}{\rho_{Hr}}$
$X_3 = \delta$	$X_4 = \phi_c$	$X_{1p} = \frac{[C_M]_p}{\rho_{Mr}}$	
$A_1 = \frac{\rho_{Mr}}{\rho_{par}}$	$A_2 = \frac{\rho_{Hr}}{\rho_{par}}$	$A_3 = \frac{\rho_{cf}}{\rho_{par}}$	$\theta = \frac{V_R}{Q}$
$B_1 = \frac{\rho_{M1}}{\rho_{Mr}}$	$B_2 = \frac{\rho_{M1}}{\rho_{par}}$	$D_{ap} = t_R\ k_p\ [N^*]_0$	
$f_c = \frac{q_{cf}}{\rho_{cf}\ V_R}$	$f_H = \frac{q_{Hf}}{\rho_{Hr}\ V_R}$	$f_I = \frac{\gamma_I}{k_{dU}}$	$\gamma_I = k_I\ [CO]$
$\gamma_H = \frac{k_{trH}}{k_p}\sqrt{\frac{M_{wM}}{\rho_{Hr}}}$	$\delta_1 = \frac{k_{dM}}{k_{dU}}\frac{\rho_{Mr}}{M_{wM}}$	$\delta_2 = \frac{k_{dH}}{k_{dU}}\sqrt{\frac{\rho_{Hr}}{M_{wH}}}$	
$\mu_1 = \frac{k^*_{HM} M_{wM}}{\rho_{Mr}}$	$\mu_2 = k^*_{HM} RT$	$\mu_3 = \frac{B\ \rho_{Mr}}{M_{wM}}$	$\mu_4 = \frac{M_{wM}\ T^{1/2}}{A\ \rho_{Mr}\ k^*_{HM}}$

The kinetic data do depend on which catalyst is used and what is composition of a catalyst. The use of different cocatalysts in a given titanium compound gives rise to different propagation rate and activation energy [Choi and Ray, 1988]. The principal reason for improving catalyst performance is to increase polymer yield and to improve the polymer morphology. Consequently, only the propagation rate constant and its activation energy are experimentally measured for a newly developed catalyst. However, to operate the polymerization reactor optimally and safely, other reaction steps already discussed should be considered. Though no published paper contains all necessary kinetic data, the use of kinetic data on similar Ziegler-Natta catalysts selected from several sources in the open literature enables a quantitative study of reactor dynamics. Physical properties and operating parameters are shown in Table 3.

Choi and Ray [1988] modeled propylene polymerization over a conventional Ziegler-Natta catalyst in a CSBR. Their operating parameters are used in this work with minor modification of some parameters, e.g., the reference pressures. Rincon-Rubio et al. [1990] used a slurry lab-scale reactor to polymerize propylene with a highly active magnesium supported Ziegler-Natta catalyst. Their model included several deactivation rate constants, though useful or valid only for an isothermal system. There are no published kinetic data for the deactivation steps. Consequently, the values for the deactivation rate constants used in this research are assumed constant for both the isothermal and nonisothermal model. If this assumption results in a significant difference between the predicted and real PSD, as a consequence of the ignorance of the nonisothermal effect, these results may still offer some guidance to the study of reactor dynamics. This model may be reasonably extended to the solution of a real nonisothermal reactor, if sufficient kinetic data are available. Chen [1993]

Table 3. Physical properties and operation parameters for olefin polymerization

Parameter	Value	Reference
ρ_{Mr}	0.093 (g/cm^3)	
ρ_{par}	0.9103 (g/cm^3)	Choi and Ray [1988]
ρ_{M1}	0.4 (g/cm^3)	Choi and Ray [1988]
ρ_{Hr}	1.625×10^{-4} (g/cm^3)	
ρ_{cf}	2.84 (g/cm^3)	Chen [1993]
V_0	6.545×10^{-8} (cm^3)	Chen [1993]
V_R	1.0×10^{6} (cm^3)	Choi and Ray [1988]
$[N^*]_0$	6.0×10^{-6} (mol/cm^3 cat)	
[CO]	1.0×10^{-5} (mol/cm^3)	
k_p	3.948×10^{9} (cm^3/mol hr)	Rincon-Rubio et al. [1990]
k_I	7.094×10^{10} (cm^3/mol hr)	Chen [1993]
k_{trH}	3.0525×10^{5} (cm$^{3/2}$/mol$^{1/2}$ hr)	Rincon-Rubio et al. [1990]
k_{dU}	0.066 (*l*/mol)	Rincon-Rubio et al. [1990]
k_{dM}	23.7 (cm^3/mol hr)	Rincon-Rubio et al. [1990]
k_{dH}	4.773 (cm$^{3/2}$/mol$^{1/2}$ hr)	Rincon-Rubio et al. [1990]
ε	0.25	Choi and Ray [1988]
T_r	300.15 (K)	Choi and Ray [1988]
T_f	328.15 (K)	Choi and Ray [1988]
P_{Mr}	22 (atm)	
P_{Hr}	2 (atm)	Srinivasan et al. [1988]

Table 4. Chain transfer rate constants and the ratio of chain transfer constant to propagation rate constant

	k_{trH} $\left(\frac{cm^{3/2}}{mol^{1/2}\,hr}\right)$	Reaction temperature	Catalyst	$\frac{k_{trH}}{k_p}$
Yuan et al. [1982]	2.95×10^{13}		A	2.24×10^{2}
Bosworth [1983]	1.138×10^{6}		Supported catalyst	6.33×10^{-4}
Rincon-Rubio et al. [1990]	3.0525×10^{5}	70 °C	B	0.77×10^{-4}
Sarkar and Gupta [1992, 1993]	6.69×10^{5}	70 °C	A	3.72×10^{-4}
Choi [1984]	2.41×10^{9}	87 °C	δ $TiCl_3$ type	1.1×10^{4}
Kuo [1985]	1.59×10^{4}	50 °C	C	0.59×10^{-4}
Galvan [1986]	3.60×10^{6}		$TiCl_4/MgCl_2$ type	1.0×10^{-4}

where A: δ $TiCl_3/AlCl_3$/TEA, B: $TiCl_4/MgCl_2$/TEA/DMS, C: $TiCl_4/MgCl_2$/EB/PC/DMS
*This value is a pre-exponential factor (Activation Energy = 12 kcal/mol)

Table 5. The general solution of a reaction system for an isothermal olefin polymerization

$$X_1=\frac{B_1+\frac{t_R}{A_1}\left(A_3 f_c-\frac{1-\varepsilon}{\theta}\right)}{\frac{t_R\,\varepsilon}{\theta}}$$

$$f_H-\frac{X_2\,\varepsilon}{\theta}+\frac{X_2^{1/2}\,\gamma_H}{A_1 X_{1p}}\left(A_3 f_c-\frac{1-\varepsilon}{\theta}\right)=0$$

$$X_3=\frac{\frac{t_R}{A_3}\left(-A_3 f_c+\frac{1-\varepsilon}{\theta}\right)}{D_{ap}\,X_{1p}\int_{V_c}^{\infty}\frac{\bar{i}f}{[N]_0^*}dv}$$

$$X_4=\frac{A_3 f_c}{(1-\varepsilon)/\theta}$$

Table 6. The general solution of a nonisothermal reactor system for olefin polymerization

$$X_1=\frac{B_1+\frac{t_R}{A_1}\left(A_3 f_c-\frac{1-\varepsilon}{\theta}\right)}{\frac{t_R\,\varepsilon}{\theta}}$$

$$f_H-\frac{X_2\varepsilon}{\theta}+\frac{X_2^{1/2}\,\gamma_H}{A_1 X_{1p}}\left(A_3 f_c-\frac{1-\varepsilon}{\theta}\right)=0$$

$$X_3=\frac{\frac{t_R}{A_3}\left(-A_3 f_c+\frac{1-\varepsilon}{\theta}\right)}{D_{ap}\,X_{1p}\int_{V_c}^{\infty}\frac{\bar{i}f}{[N]_0^*}dv}$$

$$X_4=\frac{A_3 f_c}{(1-\varepsilon)/\theta}$$

$$X_5=\frac{L_f-\frac{t_R\,A_3}{B_1\,A_1}[BH_R+(A_4-1)]\,f_c}{\left(1+f_R-\frac{t_R(1-A_4)(1-\varepsilon)}{B_1\,A_1\,\theta}\right)+\frac{t_R\,A_3(1-A_4)}{B_1\,A_1}\,f_c}$$

$$L_f=(1+f_R)(1-BH_v)+A_5[f_R(X_{5R}-1)+(X_{5f}-1)]+\frac{t_R\,BH_R(1-\varepsilon)}{B_1\,A_1\,\theta}-\frac{t_R(1-A_4)(1-\varepsilon)}{B_1\,A_1\,\theta}$$

measured the kinetics of propylene polymerization in a gas phase lab-scale reactor with magnesium chloride-supported Ziegler-Natta catalyst similar to Rincon-Rubio et al. [1990]. These data are used in our nonisothermal model, since it requires activation energy data. No one, however, has measured the activation energy for chain transfer to hydrogen, k_{trH}. Although the amount of hydrogen injected to the reactor is small and the main purpose of hydrogen is molecular weight control, the rate change of the hydrogen concentration in the reactor is important because of the hydrogen-assisted deactivation at the particle. An estimate of the rate constant and activation energy for k_{tH} was obtained from the ratio, k_{trH}/k_p, calculated from several experimental data (Table 4). Most values of the ratio are near 10^{-} and it is used in this study. From k_p and activation energy for propagation [Chen, 1993] and the transfer ratio, the chain transfer rate constant for a nonisothermal system was estimated.

Algebraic manipulation of the governing equations for the isothermal system leads to the solution given in Table 5. The principal parameter of the olefin polymerization model is not the residence time of monomer but the catalyst injection rate. Since mass and heat transfer resistances are negligible and bed height is a variable, the governing equations can be combined. Inserting the total PSD function derived in Kim et al. [1997] into the solution, the reactor dynamics and the effect of PSD can be recovered for each given reaction mechanism.

The solution form of a nonisothermal system is shown in Table 6. Note that catalyst ignition and extinction phenomena are assumed to be negligible and the mixing of particles is ideal.

FEASIBLE REGIONS CONSTRAINTS

There are several physical constraints for feasible polymer reactor operation. These are derived from dimensionless variables and thermodynamics. Since the definition of bed height is the ratio of polymer particle volume to reactor volume, this dimensionless variable has a range between zero and one. For simplicity, the derivation presented is confined to the simple reaction mechanism model. Inserting the total PSD function into the model solution of X_3, the following constraints are derived.

For $X_3 \geq 0$, $\Theta \leq \frac{1-\varepsilon}{A_3 f_c}$

$$\text{For } X_3 \le 1,\ \Theta \ge \frac{1-\varepsilon}{A_3 f_c + \dfrac{A_1 D_{ap} f_c f_I}{t_R \gamma_I \delta_I}} \tag{3}$$

The dimensionless monomer concentration, X_1, should be greater than zero, for the monomer is not completely depleted during polymerization.

$$\text{For } X_1 \ge 0,\ \Theta \ge \frac{1-\varepsilon}{A_3 f_c + \dfrac{A_1 B_1}{t_R}} \tag{4}$$

For the calculation of the monomer concentration at the particle, the Redlich-Kwong (RK) equation of state is used. X_{1p}, which is the ratio of monomer concentration at the particle to the reference concentration, should be greater than zero. The dimensionless RK equation can be expressed by

$$X_{1p} = \frac{\mu_2}{\dfrac{1}{X_1} - \mu_3} - \frac{1}{\dfrac{\mu_4}{X_1}\left(\dfrac{1}{X_1} + \mu_3\right)} \tag{5a}$$

The denominator of the attraction term of the RK equation has to be greater than zero to avoid a negative pressure.

$$\text{For } X_1 \le \frac{1}{\mu_3},\ \Theta \le \frac{t_R\left(\dfrac{1-\varepsilon}{A_1} + \dfrac{\varepsilon}{\mu_3}\right)}{B_1 + \dfrac{t_R A_3 f_c}{A_1}} \tag{5b}$$

Since propylene injected into the reactor absorbs heat of polymerization and vaporizes, there is no condensation of monomer. The propylene pressure, therefore, must be less than the vapor pressure, P_M^*.

$$\text{For } P_M \le P_M^*,\ \Theta \le \frac{t_R\left(\dfrac{1-\varepsilon}{A_1} + \dfrac{\varepsilon \mu_2 \mu_4}{2}\right)}{B_1 + \dfrac{t_R A_3 f_c}{A_1}} \tag{6}$$

These five constraints define a feasible region of reactor operation with constant withdrawal rate. If the bed height is controlled and fixed, i.e., the volumetric withdrawal rate is not fixed, these constraints may not be valid. Bed height, however, is much more difficult to control than the withdrawal rate, since the withdrawal rate must vary in order to control bed height. The consequence may be an irregular production of polymer.

RESULTS AND DISCUSSION

1. Feasible Operating Regions

The constraints developed above define the feasible region within which the polymerization reactor may be operated. Fig. 3 shows the five restrictions and that the dimensionless withdrawal rate must decrease with increasing catalyst injection rate (for the simple reaction mechanism model with t_R=1 hr). The feasible operating range lies in the bounded region between the line, $X_3 \ge 0$ and the constraint, $X_3 \le 1$. More severe restrictions, however, lie within the bounded region. The expanded diagram in Fig. 3 shows the more restrictive operability region surrounded by $X_1 \ge 0$ and PR < PR*. A plot of volumetric withdrawal rate versus catalyst injection rate (Fig. 3) is drawn for the simple reaction mechanism model with 1 hour monomer residence time. The catalyst residue in polymer particles increases with increasing catalyst injection rate. A significant catalyst residue may result in undesirable products. Therefore, it must be as low as possible. The feasible region of operation may be confined to a volumetric withdrawal rate between 0.575 and 0.585 (m^3/hr).

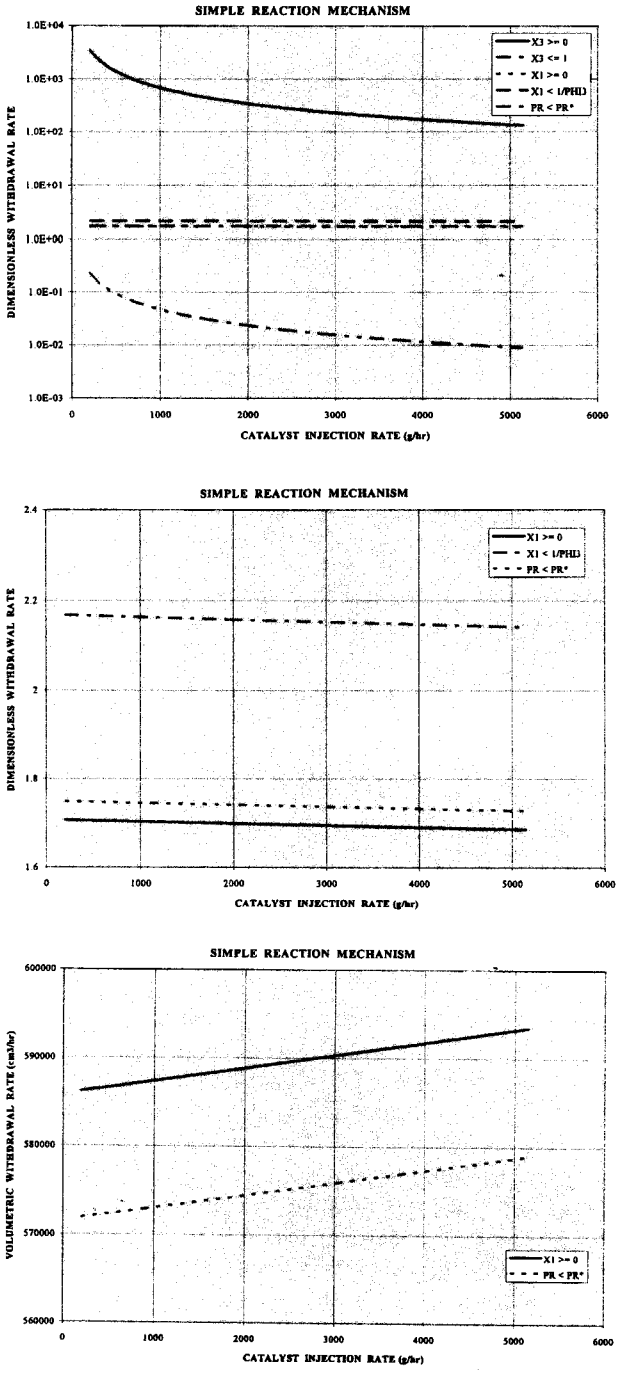

Fig. 3. Feasible operating regions for a simple reaction model.

2. Simple Reaction Mechanism

Fig. 4 shows steady state profiles of monomer concentration, hydrogen concentration, bed height, catalyst residue and monomer pressure for 1 hour monomer residence time. Note that monomer and hydrogen concentrations increase with an increase in catalyst injection rate, which means that less monomer and hydrogen are consumed by a greater catalyst injection. This is due to the fixed polymer withdrawal rate. The general solution of the isothermal system shown in Table 5 leads to this conclusion. Since θ and t_R are fixed and B_1 is a given feed concentration of monomer, the monomer bulk concentration is proportional to the catalyst injection rate. If the catalyst feed increases, the bed height described in Eq. (6) decreases.

$$X_3 = \frac{\frac{t_R}{A_3}\left(-A_3 f_c + \frac{1-\varepsilon}{\theta}\right)}{D_{ap} X_{1p} \int_{V_c}^{\infty} \frac{\bar{i} f}{[N]_0^*} dV} = \frac{B_1 - \frac{X_1 t_R \varepsilon}{\theta}}{D_{ap} X_{1p} \int_{V_c}^{\infty} \frac{\bar{i} f}{[N]_0^*} dV} \qquad (7)$$

If $f_c \rightarrow 0$

larger amount of X_1 in the reactor

X_1 is withdrawn (for θ fixed) and X_3 is larger.

If $f_c \rightarrow \infty$,

larger amount of f_c in the reactor

f_c is withdrawn (for θ fixed) and X_3 is smaller.

The catalyst residue and monomer concentration also increase with catalyst injection rate. The increase in mean number volume and diameter with increasing catalyst injection can be explained by showing that the average volume growth depends on the propagation step and that mean volume is linearly proportional to the monomer concentration at the particle, X_{1p}. Since monomer pressure is related to X_{1p} by Stern's correlation and the pressure increases with catalyst injection rate, the mean volume and diameter are greater for a larger catalyst injection rate. In Fig. 5 is shown the change of polymer yield with catalyst injection rate. The reason that polymer yield decreases with higher catalyst injection rate can be understood by Eq. (6). For larger catalyst concentration in the reactor at a fixed volumetric withdrawal rate, much more catalyst is withdrawn. At a low monomer concentration, the propagation reaction rate will be smaller than at a higher monomer concentration, or correspondingly, a smaller catalyst injection rate. Choi and Ray [1985] summarized polymer yields for different catalyst systems. Most reported data are observed not in commercial scale continuous reactors but in lab-scale batch reactors. Recently developed new generation catalysts have yields greater than 4000 (g polymer/g catalyst) in lab-scale reactors. Yields of 1200-2000 (g polymer/g catalyst), however, may be reasonable for most catalysts in com-

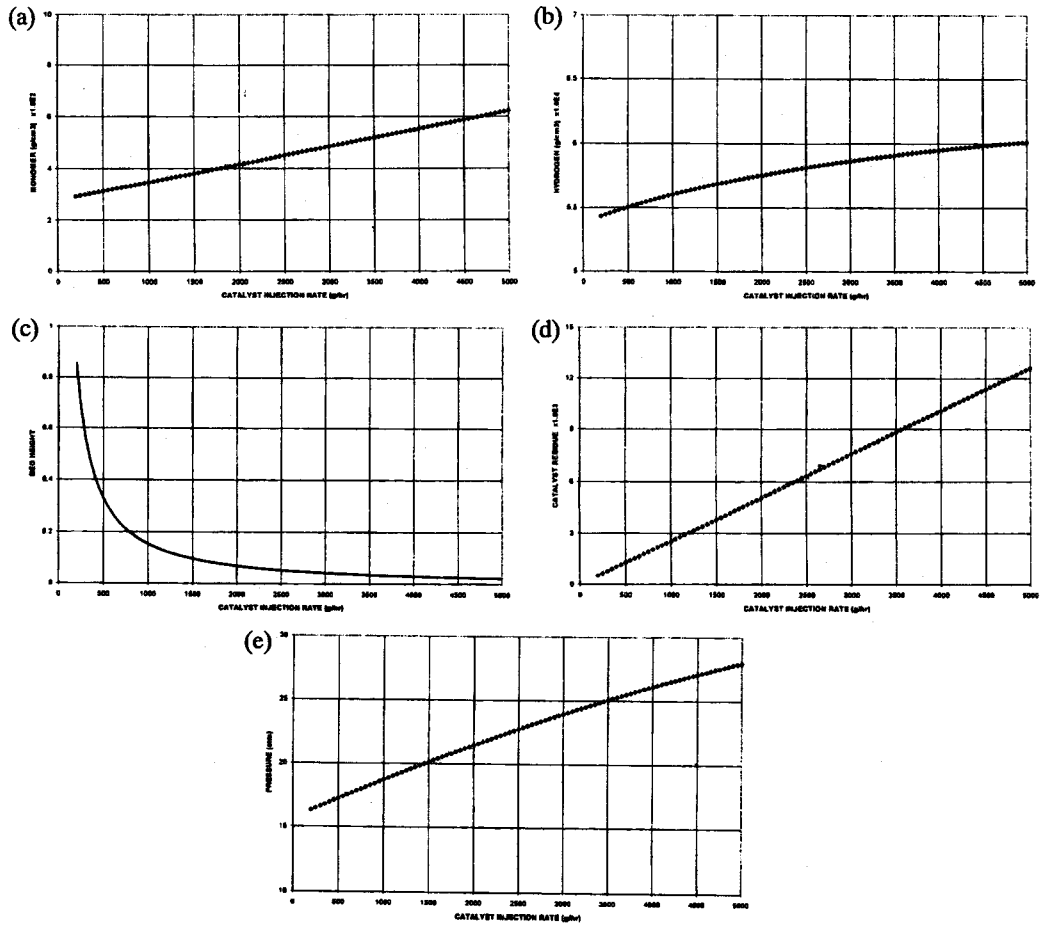

Fig. 4. Steady state profiles for a simple reaction mechanism with 1 hr monomer residence time.

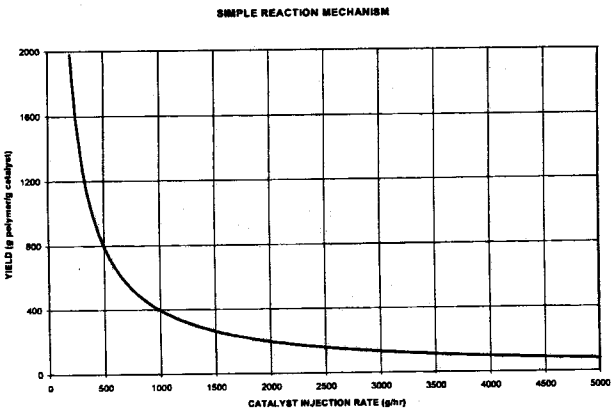

Fig. 5. Polymer yield with catalyst injection rate for a simple reaction mechanism.

mercial scale reactors.

The effect of catalyst injection rate on total particle size distribution is shown in Fig. 6. When the catalyst injection rate, q_{cf}, increases, as expected, more particles are made and the total PSD becomes much broader. The peak of each PSD slightly shifts to a larger size for an increase in q_{cf}. Since the reactor is assumed to be well-stirred, the shape of the total PSD resembles that of the residence time distribution, an exponential decay. However, the curves describing a normalized distribution (the total PSD divided by q_{cf}) plotted in Fig. 7, do not superpose. The PSD curve depends not only on the residence time distribution, but also on the reaction. We can see the PSD is a function of average number of active sites which depends on the reaction mechanism and the residence time distribution. The cumulative PSD is drawn in Fig. 7. The slope of the cumulative curve is steep for higher q_{cf}. Tait [1989] plotted the cumulative distribution using experimental data and showed that a mean value of the diameter is approximately 0.1 cm. A mean diameter of the particle of around 0.1 cm was also reported by Karol [1984]. The cumulative PSD calculated in this model also shows that a mean diameter of the particle is about 0.1 cm. The average number of active sites, the ratio of initiation step to deactivation step, is inversely proportional to the monomer concentration. Therefore, it decreases for higher catalyst injection rate, as seen in Fig. 8.

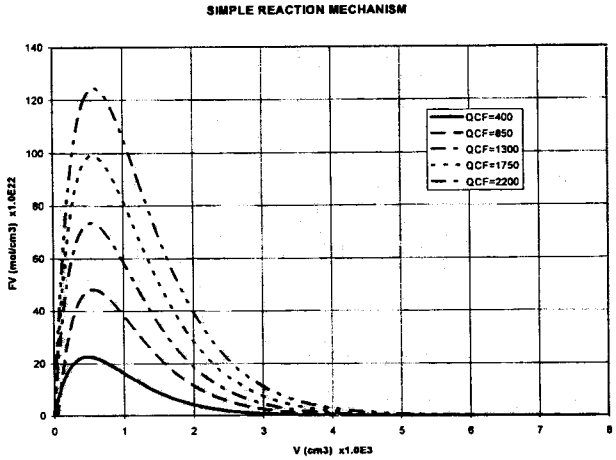

Fig. 6. The Effect of catalyst injection rate on particle size distribution for a simple reaction mechanism.

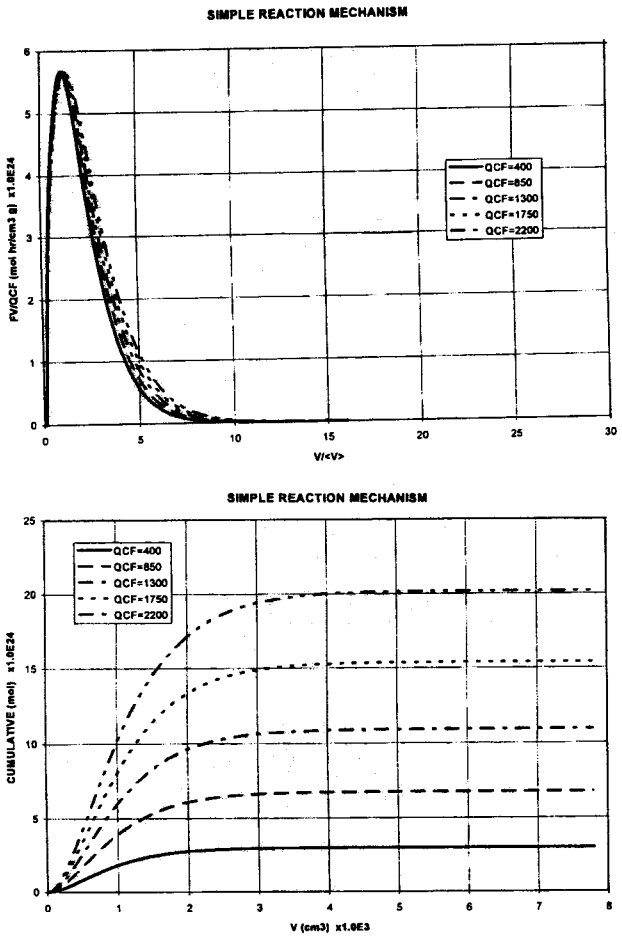

Fig. 7. Particle size distribution curves for a simple reaction mechanism.

In order to check the stability of a steady state solution, the eigenvalues of the governing equations for an isothermal system are analyzed. One of the four eigenvalues is positive in a feasible operating region, that is, 300-700 g/hr catalyst injection rate. That steady state is unstable. Without the help of a controller, stable reactor operation is impossible. PID control or nonlinear model predictive control may be useful to control the reactor [Bequette, 1991]. The effect of reactor temperature on the behavior of steady state will be described in a later section.

3. Active Site Reduction Mechanism

Kuo [1985] found that the termination of active sites follows second order kinetics at higher and lower aluminum/titanium ratios in their high-mileage Ziegler-Natta catalyst. The following expression of termination rate constant was obtained using their data.

$$k_T = 1.429 \times 10^5 \exp\left(-\frac{E_T}{RT}\right) \quad \left(\frac{1}{\text{mol sec}}\right) \tag{7}$$

This value, however, appears unreasonable, given the performance of a commercial reactor at a reasonable reaction temperature, T=343.15 K. Given these data, we cannot operate

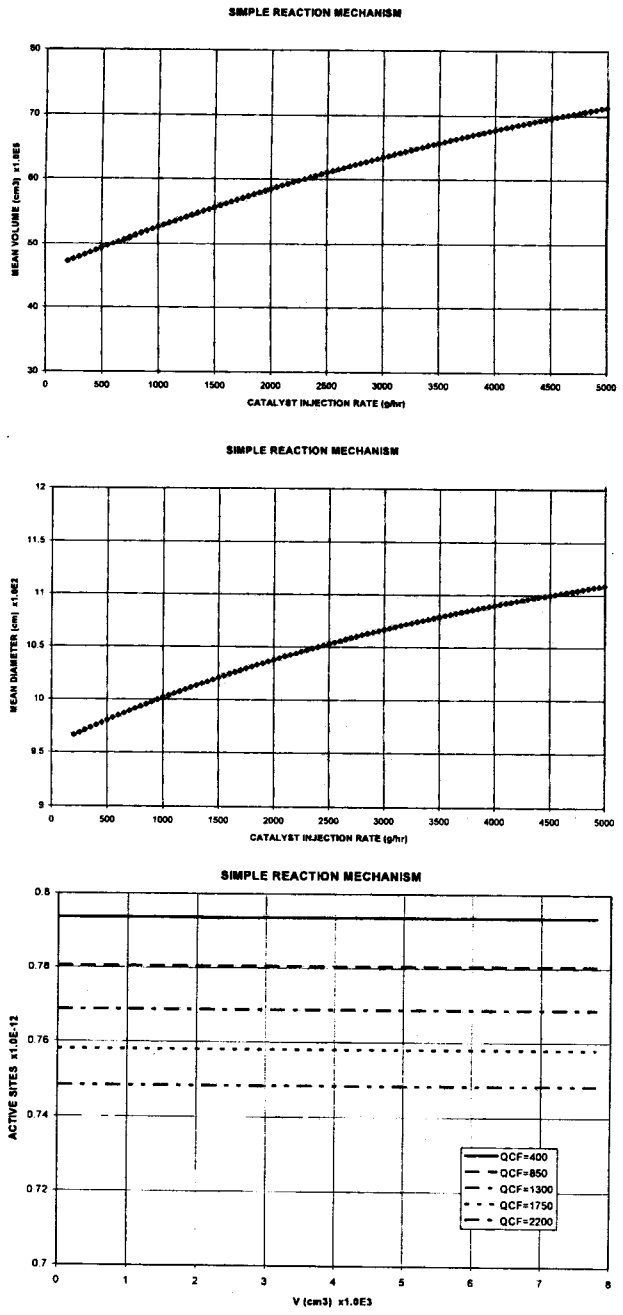

Fig. 8. Mean particle volume and diameter and average number of active sites for a simple reaction mechanism.

the reactor below a 3 kg/hr catalyst injection rate, and the polymer yield is too low. To understand the effect of an active site reduction mechanism on the reactor dynamics, the value of termination rate constant is assumed to be 3.36×10^5 (cm^3/mol hr). Note that from the governing equations of this model, the solution does depend strongly on the value of k_T. Combining the solution form with particle size distribution function, the following relation can be derived.

$$X_3 = \frac{\left(-A_3 f_c + \dfrac{1-\varepsilon}{\theta}\right)}{f_c}$$

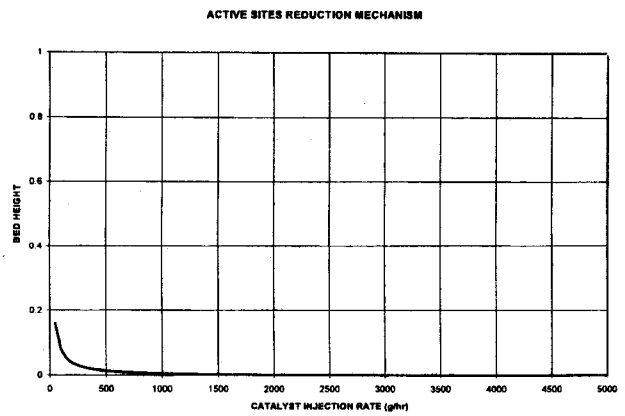

Fig. 9. Bed height vs. catalyst injection rate for active site reduction mechanism.

$$\left[\frac{\dfrac{4\,t_R^2}{\theta^2 X_{1p} A_1^2}\left\{\dfrac{2\gamma_t}{D_{ap}}\left(\dfrac{1+\gamma_t\,\theta}{f_I}\right)\right\}}{\dfrac{2t_R}{\theta X_{1p} A_1}\sqrt{\dfrac{2\gamma_t}{D_{ap}}\left(\dfrac{1+\gamma_t\,\theta}{f_I}\right)}+1}\right] \tag{8}$$

where $\gamma_t = k_t/k_p$

Since monomer and hydrogen concentrations are not affected by k_T, the trends with catalyst injection rate are the same as those of simple model case. Bed height, however, changes dramatically when compared to simple reaction model. The bed height is always lower than 0.2 for all catalyst injection rate as shown in Fig. 9. Lower bed height shows that total particle volume is small. From Eq. (8) we can see that X_3 is strongly sensitive to γ_t with fixed t_R and θ for a given f_c. For a larger γ_t, bed height becomes higher and conversely, bed height is lower for a small γ_t.

The total particle size distribution and cumulative PSD are depicted in Kim et al. [1997]. Note that the peak maximum is lower than that in a simple model for all given q_{cf} values and the distribution is broader. Since the termination reaction occurs between two growing polymers in the particles [Kuo, 1985], the sizes of the particles differ, each having a different growth path. The average number of active sites does not change with catalyst injection rate. These depend on not only particle volume, but also the termination rate constant. In contrast to a simple model case where the average number of active sites is constant, the average number of active sites in this model is proportional to the square root of the particle volume. This is a consequence of the termination step. Min [1976] and Rawlings [1985], studying emulsion polymerization, showed that the average number of radicals in the particles can be obtained from the Stockmayer-O'Toole equation, which consists of the termination mechanism and radical entry into the particle and radical exit from the particle. Unlike the radical transfer step in emulsion polymerization, all active sites remain in the particle, and the total number of sites involving potential and dead sites is conserved in olefin polym-

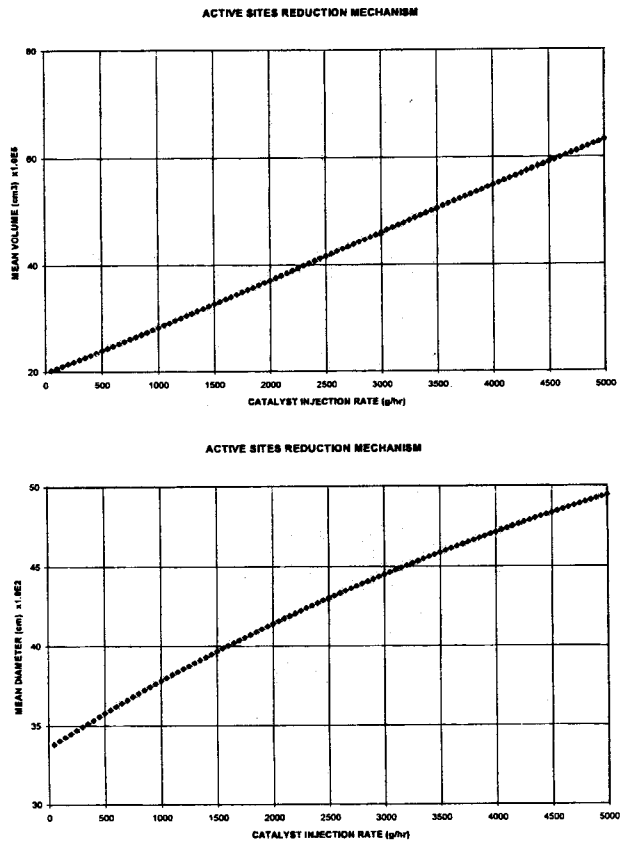

Fig.10. Mean particle volume and diameter for active site reduction mechanism.

erization. Mean number volume and diameter are drawn in Fig. 10. These values are surprisingly large and unrealistic for current catalyst systems. Since Kuo [1985] used a lab-scale batch reactor to polymerize propylene over high-mileage Ziegler-Natta catalyst, this termination kinetic data may not be entirely relevant for commercial scale reactors. Although the results shown in this model are not appropriate for a commercial process, we may still use this model to understand whether newly made or improved catalysts have the termination mechanism. Rincon-Rubio et al. [1990] modeled active site transformation as a first order mechanism for their batch slurry system. Since its transformation of active sites is very similar to an unassisted deactivation mechanism, we could include it as an extension of a simple model readily if it were important for a specific catalyst.

4. Nonisothermal System

In the study of the thermal effects on the reactor dynamics and particle size distribution, a simple reaction mechanism with a single type active site is used. The additional dimensionless groups are defined in Table 7. The general solution of a nonisothermal system is given in Table 6. Note that the Henry's constant is also a function of temperature and expressed as follows:

$$k^*_{HM} = 10^{-\left[5.38 - 1.08\left(\frac{Td}{X_s}\right)^2\right]} \tag{9}$$

A classical van Heerden analysis, a comparison of the heat

Table 7. Additional dimensionless groups for a nonisothermal reactor system

$X_5 = \frac{T}{T_{ref}}$	$f_R = \frac{q_R}{q_{Mf}}$	$X_{5R} = \frac{T_R}{T_{ref}}$
$A_4 = \frac{C_{ppar}}{C_{pM}}$	$A_5 = \frac{C_{pM1}}{C_{pM}}$	$X_{5R} = \frac{T_{fM}}{T_{ref}}$
$BH_R = \frac{(-\Delta H_{rxn})}{C_{pM}\, T_{ref}}$	$BH_v = \frac{(\Delta H_v)}{C_{pM}\, T_{ref}}$	$T_d = \frac{T_{cr}}{T_{ref}}$

generation and removal terms, affords a check of the stability of steady state solutions. Heat generation (HG) contains the reaction terms which generate heat of reaction. Heat removal (HR) is effected by the convection of monomer (recycled and fresh) and the vaporization of liquid monomer feed.

$$HG = (-\Delta H_{rxn})r_M + (C_{pM} - C_{ppar})\, r_M$$
$$HR = -C_{pM1}\, q_R (T_R - T_{ref}) - C_{pM1}\, q_{Mf} (T_{fM} - T_{ref}) + (q_{Mf} + q_R)\, C_{pM} (T - T_{ref}) + (\Delta H_v)(q_{Mf} + q_R) \tag{10}$$

The general solution form of X_5 in Table 5 can be written as

$$X_5 = \frac{Z_1 - Z_2 f_c}{Z_3 + Z_4 f_c}$$

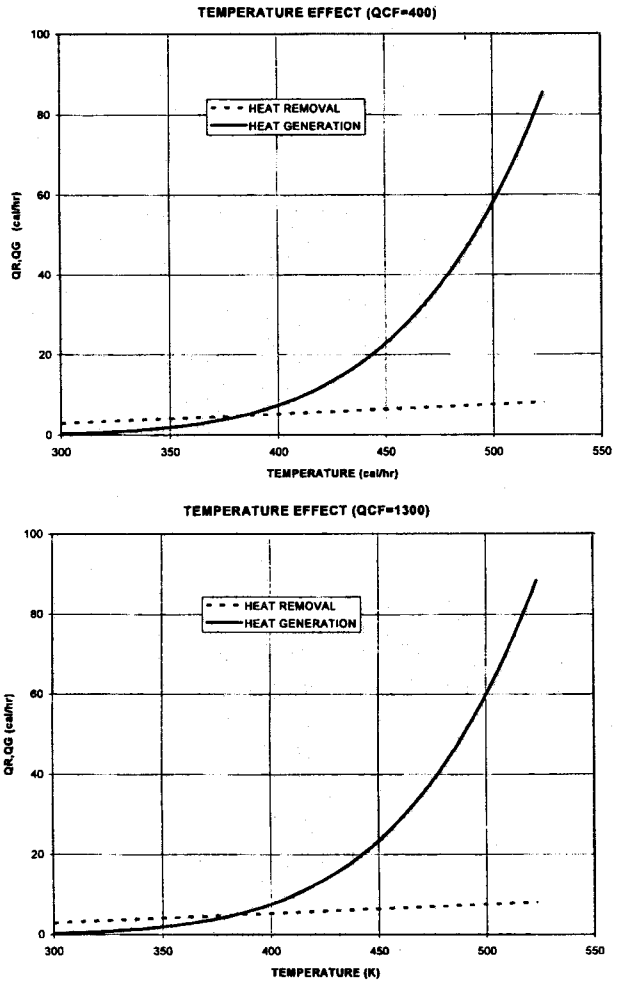

Fig. 11. Heat removal and generation curves with changing catalyst injection rate.

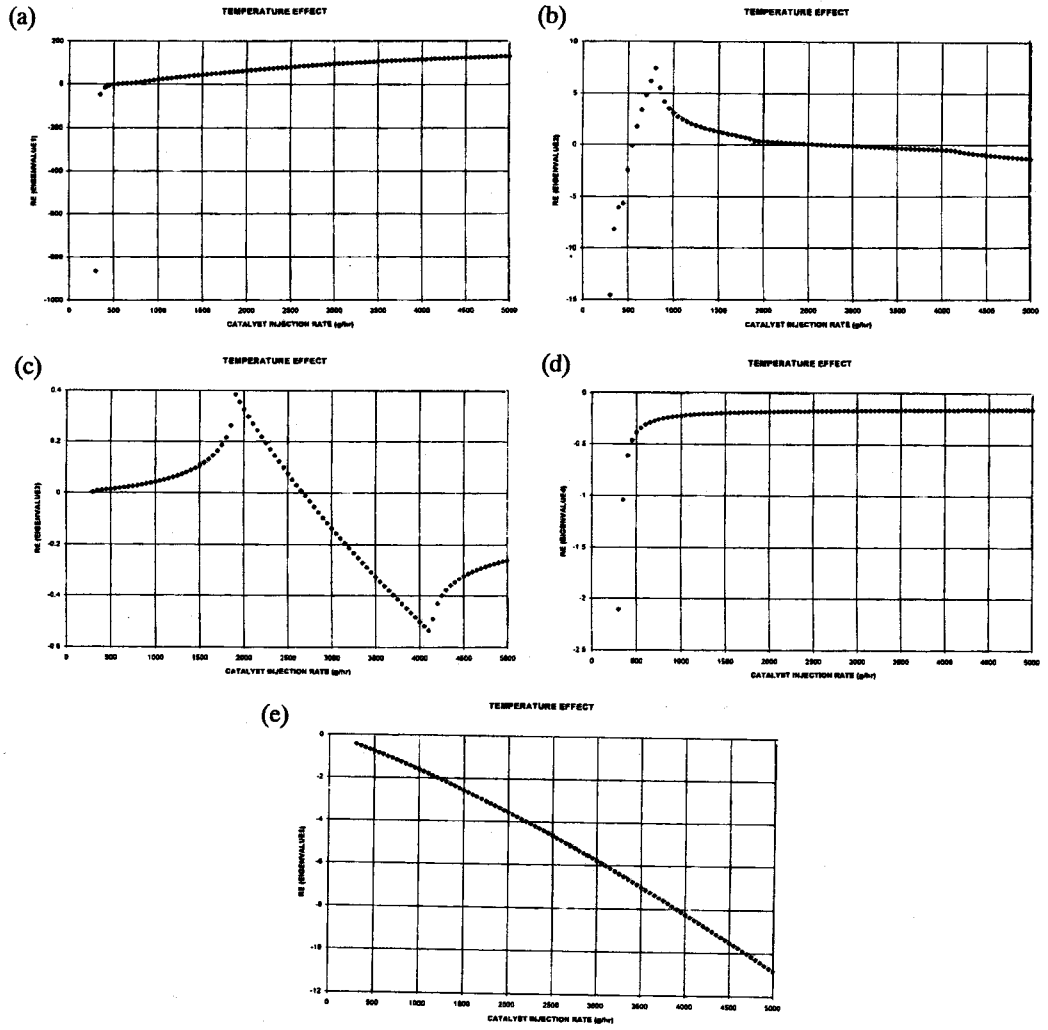

Fig. 12. Eigenvalues of steady state governing equations for a nonisothermal reactor system.

The derivative of X_5 with respect to f_c is negative, that is, $dX_5/df_c < 0$ only if $Z_3Z_2 + Z_1Z_4 > 0$. Since $Z_3Z_2 + Z_1Z_4 \neq 0$ for the data used in this work, there are no multiple steady state solutions. This unique steady state solution is seen in the plot of heat generation and removal terms as a function of catalyst injection rate (van Heerden plot). Fig. 11 shows the unique and unstable steady state which violates the Aris criterion [Aris, 1958] over the temperature range of interest. The eigenvalues are depicted in Fig. 12. For catalyst injection rate in the range of 500 to 100 (g/hr), three out of five eigenvalues are positive and, therefore, the steady state is unstable. Choi and Ray [1988] showed that one of the eigenvalues for their equations is positive and concluded that the unique steady state solution is unstable. They assumed a uniform particle size distribution and the Ideal Gas law for monomer. Consequently, eigenvalues of their model are not the same in this work. They observed a pseudo-stable region where the system exhibits only weak instability, since only one eigenvalue is positive and very small in the region. However, we find three positive eigenvalues that are not small. We conclude that there is only one unstable steady state in a nonisothermal continuous stirred-bed reactor for the polymerization of propylene over a Ziegler-Natta catalyst containing one type of active site.

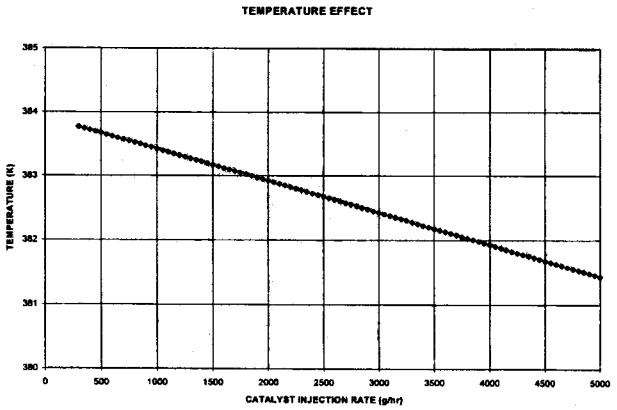

Fig. 13. Temperature variations with changing catalyst injection rate.

The monomer concentration profile in the bulk is not affected by the temperature variation during polymerization. From the general solution, we note that X_1 only depends on f_c for a fixed θ. The hydrogen concentration and bed height are changed slightly in comparison with an isothermal system. Note

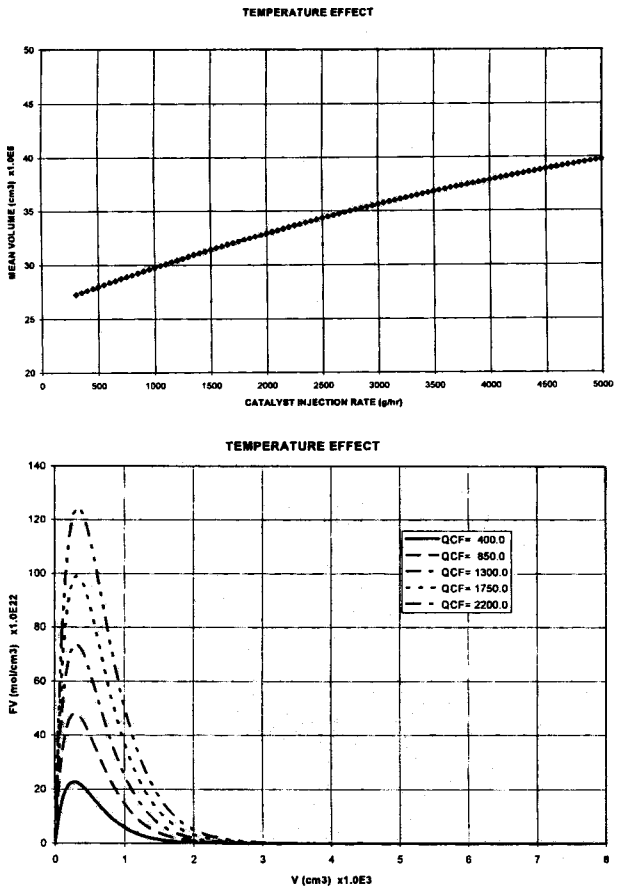

Fig. 14. Number average particle volume and total particle size distribution for a nonisothermal reaction.

that bed height is strongly dependent on the particle size distribution, determined by reaction mechanism. The dearth of kinetic data for deactivation forces us to assume that deactivation rates do not change appreciably with temperature. This assumption is acceptable, however, because the temperature variation with changing catalyst injection rate is small as shown in Fig. 13. The temperature difference at the operating region of interest is only 2 °C. Mean volume and the total PSD are drawn in Fig. 14. The mean number volume of particles in this nonisothermal case is smaller than that in an isothermal case, because the value of propagation rate constant is different. Note that <V> depends mainly on propagation reaction term and on the initial catalyst volume. In the isothermal case, we used the propagation rate constant in Rincon-Rubio et al. [1990]. On the other hand, Chen's datum [1993] is used in the nonisothermal case, since it contains an activation energy for the propagation step. The total PSD becomes much narrower and depends not only on the reaction mechanism but also the residence time distribution.

CONCLUSION

Mass and energy balances were derived for a gas-phase polymerization of propylene in a continuous stirred-bed reactor. The Redlich-Kwong equation was used to calculate monomer pressure at a given concentration. The general solutions for isothermal and nonisothermal systems were developed, setting the volumetric withdrawal rate as fixed. Our observations were:

1. Bed height and particle volume are affected by the PSD whose form depends on the reaction mechanism.
2. The feasible region for the reactor operation was calculated using physical constraints. It shows the regions of operability and of avoiding to operate the reactor.
3. The temperature change in the reactor with increasing catalyst injection rate was observed to be minimal.
4. There is only one unstable steady state solution in a propylene polymerization reactor.

For the first time, a PSD for propylene polymerization in a continuous stirred-bed reactor was derived by using reaction mechanisms. The reactor dynamics studied here will help to establish better operating conditions for increasing productivity and improving polymer properties.

NOMENCLATURE

BH : heat generation parameter
C_i : concentration of species i
CO : cocatalyst concentration
C_{pi} : heat capacity of species i
C_{pM1} : heat capacity of liquid propylene
D_{a1} : Damköhler number, i=d, p, t
E_i : activation energy of species i
F : total particle size distribution [mol/cm^3]
F_i : molar flow rate of species i
f (V, t) dV : total particle size distribution function in a volume V to V+dV at time t
H_2 : hydrogen concentration
HG : heat generation
HR : heat removal
$(-\Delta\tilde{H}_r)$: heat of reaction
ΔH_v : heat of vaporization
$\bar{i}$: average number of active sites
J : Jacobian of a matrix
k_H^* : Henry's constant
k_p : rate constant for propagation
k_{trH} : rate constant for chain transfer to hydrogen
M : monomer concentration
M_{wM} : molecular weight of monomer
N : potential sites
N_A : Avogadro's number
P : pressure
P_M : monomer pressure
Q : volumetric withdrawal rate
q_{cf} : catalyst injection rate
q_r : recycle rate
R : gas constant
r_M : rate of monomer consumption
r_p : polymer mass growth rate
r_{trH} : rate of hydrogen chain transfer
r_v : rate of particle growth [cm^3/hr]
T : reaction temperature

T_t : time
V : particle volume
V_R : reactor volume for olefin polymerization

Greek Letters

δ : fractional volume of stirred-bed
ε : ratio of gas withdrawal rate to product withdrawal rate
ϕ_c : catalyst residue
ρ_{cf} : catalyst density
ρ_i : density of species i
ρ_{par} : particle density
θ : residence time
τ : dimensionless time

Subscripts

c : catalyst
f : feed
H : hydrogen
M, m : monomer
o : initial
p : particle
R : recycle

Superscript

* : initial condition

REFERENCES

Aris, R., "Elementary Chemical Reactor Analysis", Prentice-Hall, Englewood Cliffs, New Jersey (1969).

Bequette, B. W., "Nonlinear Control of Chemical Processes: A Review", *Ind. Eng. Chem. Res.*, **30**, 1391 (1991).

Bosworth, D. J., "The Mathematical Modelling of Gas-Phase Polymerization Reactors", Ph.D. Thesis, Univ. of London (1983).

Brockmeier, N. F. and Rogan, J. B., "Simulation of Continuous Propylene Polymerization in a Backmix Reactor Using Semibatch Kinetic Data", *AIChE Symp. Ser.*, **72**(160), 28 (1976).

Chen, C. M., "Gas Phase Olefin Copolymerization with Ziegler-Natta Catalysts", Ph. D. Thesis, Univ. of Wisconsin, Madison (1993).

Choi, K. Y., "The Reaction Kinetics, Modeling and Control of Solid Catalyzed Gas Phase Olefin Polymerization Reactors", Ph.D. Thesis, University of Wisconsin, Madison (1984).

Choi, K. Y. and Ray, W. H., "Recent Developments in Transition Metal Catalyzed Olefin Polymerization-A Survey. II. Propylene Polymerization", *JMS-Rev. Macromol. Chem. Phys.*, **C25**(1), 57 (1985).

Choi, K. Y. and Ray, W. H., "The Dynamic Behavior of Continuous Stirred-Bed Reactors for the Solid Catalyzed Gas Phase Polymerization of Propylene", *Chem. Eng. Sci.*, **43** (10), 2587 (1988).

Floyd, S., Choi, K. Y., Taylor, T. W. and Ray, W. H., "Polymerization of Olefins through Heterogeneous Catalysis. III. Polymer Particle Modelling with an Analysis of Intraparticle Heat and Mass Transfer Effects", *J. Appl. Poly. Sci.*, **32**, 2935 (1986a).

Floyd, S., Choi, K. Y., Taylor, T. W. and Ray, W. H., "Polymerization of Olefins through Heterogeneous Catalysis. IV. Modeling of Heat and Mass Transfer Resistance in the Polymer Particle Boundary Layer", *J. Appl. Poly. Sci.*, **31**, 2131 (1986b).

Floyd, S., Heiskanen, T., Taylor, T. W., Mann, G. E. and Ray, W. H., "Polymerization of Olefins through Heterogeneous Catalysis. VI. Effect of Particle Heat and Mass Transfer on Polymerization Behavior and Polymer Properties", *J. Appl. Poly. Sci.*, **33**, 1021 (1987).

Galvan, R., "Modeling of Heterogeneous Ziegler-Natta (Co) polymerization of α-Olefins", Ph. D. Thesis, Univ. of Minnesota (1986).

Gonzalez, V., "Estimation and Control of Molecular Weight Distributions in Polymethyl Methacrylate Polymerizations", Ph. D. Thesis, Univ. of Minnesota (1990).

Hutchinson, R. A. and Ray, W. H., "Polymerization of Olefins through Heterogeneous Catalysis. VII: Particle Ignition and Extinction Phenomena", *J. Appl. Poly. Sci.*, **34**, 657 (1987).

Hutchinson, R. A. and Ray, W. H., "Polymerization of Olefins through Heterogeneous Catalysis. VIII: Monomer Sorption Effects", *J. Appl. Poly. Sci.*, **41**, 51 (1990).

Karol, F. J., "Studies with High Activity Catalysts for Olefin Polymerization", *Catal. Rev. Sci. Eng.*, **26**(3/4), 557 (1984).

Kim, J. Y., Conner, W. C. and Laurence, R. L., "Particle Size Distribution in Olefin Continuous Stirred-Bed Polymerization Reactors", submitted to *Korean J. Chem. Eng.* (1997).

Kuo, C., "Magnesium Chloride Supported High-Activity Catalyst for Olefin Polymerization", Ph. D. Thesis, University of Massachusetts, Amherst (1985).

McAuley, K. B., MacGregor, J. F. and Hamielec, A. E., "A Kinetic Model for Industrial Gas-Phase Ethylene Copolymerization", *AIChE J.*, **36**(6), 837 (1990).

Min, K. W., "The Modeling and Simulation of Emulsion Polymerization Reactors", Ph. D. Thesis, SUNY, Buffalo (1976).

Min, K. W. and Ray, W. H., "On the Mathematical Modeling of Emulsion Polymerization Reactors", *J. Macromol. Sci.-Revs. Macromol. Chem.*, **C11**(2), 177 (1974).

Rawlings, J. B., "Simulation and Stability of Continuous Emulsion Polymerization Reactors", Ph. D. Thesis, University of Wisconsin, Madison, 1985.

Reid, R. C., Prausnitz, J. M. and Poling, B. E., "The Properties of Gases and Liquids", McGraw-Hill, Englewood-Cliffs, New Jersey (1987).

Rincon-Rubio, L. M., Wilen, C. E. and Lindfors, L. E., "A Kinetic Model for the Polymerization of Propylene over a Ziegler-Natta Catalyst", *Eur. Polym. J.*, **26**(2), 171 (1990).

Sarkar, P. and Gupta, S. K., "Steady State Simulation of Continuous-Flow Stirred-Tank Slurry Propylene Polymerization Reactors", *Poly. Eng. Sci.*, **32**(11), 732 (1992).

Sarkar, P. and Gupta, S. K., "Modelling of Semibatch Polypropylene Slurry Reactor", *Polymer*, **34**(21), 4417 (1993).

Srinivasan, P. R., Shashikant, P. R. and Sivaram, S., "Hydrogen Effects in Olefin Polymerization Catalysts", *Chem. Ind.*, 723 (1988).

Tait, P. J. T., "Monoalkene Polymerization: Ziegler-Natta and

Transition Metal Catalysts", in G. Allen and J. C. Bevington ed., Comprehensive Polymer Science: The Synthesis, Characterization, Reactions & Applications of Polymers, Pergamon Press (1989).

Tait, P. J. T. and Watkins, N. D., "Monoalkene Polymerization: Mechanisms," in G. H. Allen and J. C. Bevington ed., Comprehensive Polymer Science: The Synthesis, Characterization, Reactions & Applications of Polymers, Pergamon Press (1989).

Yuan, H. G., Taylor, T. W., Choi, K. Y. and Ray, W. H., "Polymerization of Olefins through Heterogeneous Catalysis. I. Low Pressure Propylene Polymerization in Slurry with Ziegler-Natta Catalyst", *J. Appl. Poly. Sci.*, **27**, 1691 (1982).